



5-HT₇ Receptor Ligands: A 3D-QSAR CoMFA and CoMSIA Analysis of Quinazolinone Derivatives

¹Shravan Kumar. Gunda*, ¹Sandeep Kumar Mulukala Narasimha, ¹Adi Maha Laxmi Madasu, ²Shaik Mahmood

¹Bioinformatics Division, Osmania University, Hyderabad, Andhra Pradesh, India.

²Department of Botany, Nizam College, Hyderabad, Andhra Pradesh, India.

*Corresponding author's E-mail: gunda14@gmail.com

Accepted on: 12-06-2013; Finalized on: 31-08-2013.

ABSTRACT

3D-QSAR studies based on Comparative molecular field analysis (CoMFA) and comparative molecular similarity indices analysis (CoMSIA) were investigated on a series of 77 novel Quinazolinone derivatives as 5-HT₇ receptor inhibitors. The best prediction was obtained with a CoMFA standard model ($q^2 = 0.851$, $r^2 = 0.950$) and with CoMSIA combined Steric, Electrostatic, Hydrophobic and Hydrogen bond donor and acceptor fields ($q^2 = 0.850$, $r^2 = 0.945$). Both models were validated by a test set of nineteen compounds producing very good results. The structural features like physicochemical properties of ligands which contribute positively towards Steric, Electrostatic, Hydrophobic and Hydrogen bond donor fields were analyzed with the help of contour maps generated by CoMFA and CoMSIA. The information obtained from CoMFA and CoMSIA 3-D contour maps can be used for the design of Quinazolinone based analogs as 5-HT₇ receptor agents.

Keywords: CoMFA, CoMSIA, 5-HT₇, PLS, Quinazolinone, QSAR.

INTRODUCTION

5-Hydroxytryptamine/ 5-HT/ G protein- coupled serotonin belong to archetypal group A Rhodopsin-like G protein-coupled receptors (GPCRs) which are expected to have 7 trans membrane helices, 3 of each intra and intercellular loops and an extracellular amino terminus and an intracellular carboxy-terminus.¹ The true structures of these receptors remain unknown, although the crystallization of the bovine Rhodopsin receptor provides promising solution for the structures of G protein-coupled 5-HT receptors in the near future.² Functionally, the trans membrane regions serve to bind ligands, especially with endogenous ligand serotonin, the intracellular domains couple with these receptors to various intracellular functions and for the most part the extracellular domains have uncertain functional roles.³ The endogenous ligand comprises of neurotransmitter serotonin, and the presence of serotonin and its receptors in a variety of invertebrates argues for a relatively early evolutionary origin of these receptors.^{4,5}

In mammals, there are six classes of G protein-coupled 5-HT receptors, namely 5-HT₁, 5-HT₂, 5-HT₄, 5-HT₅, 5-HT₆ and 5-HT₇. Among them, 5-HT₇ receptor was most recently cloned in 1993 and is found in the brain more specifically in the hypothalamus, thalamus, hippocampus, and cortex regions. The 5-HT₇ receptor is a G-protein-coupled receptor (GPCR) protein and is found to stimulate cAMP production which activates the extracellular signal-regulated kinase (ERK) through a mechanism that is dependent on a Ras monomeric GTPase.⁶ Due to the availability of selective antagonists and, recent studies on knockout mice suggest that 5-HT₇ receptor is involved in thermoregulation, circadian rhythm, learning and memory, hippocampal signaling, sleep, and endocrine

regulation. It is unclear so as to how receptor blockade could lead to antidepressant effect.⁷ However, direct actions of antidepressants on the 5-HT₇ receptor and reversal sleep disturbances were observed in depressed patients after receptor blockade, which suggest that 5-HT₇ receptor antagonists may be sufficient to treat depression.^{8,9}

QSAR based on the 3D structures of ligands involve two methods namely CoMFA¹⁰ and CoMSIA¹¹ which provide detailed investigation of receptor- ligand interactions. Here, we describe 3D-QSAR CoMFA and CoMSIA studies performed on a series of 77 Quinazolinone derivatives. Thus, the resulting CoMFA and CoMSIA studies will not only illustrate the conformation or spatial orientation of 5-HT₇ Quinazolinone derivatives but also provide useful indicators for the design of new drug candidates for 5-HT₇.

MATERIALS AND METHODS

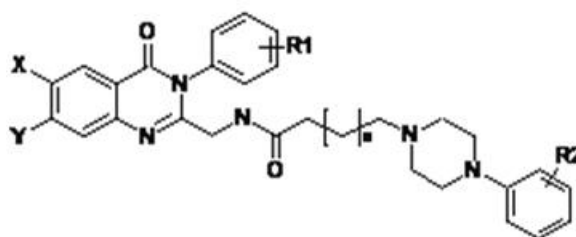
Molecular structures and optimization

A dataset of 77 Quinazolinone derivatives having a common scaffold and their inhibitory activities against 5-HT₇ were collected from literature¹² and molecules 12, 32, 36, and 49 whose IC₅₀ values reported as >10,000 were not considered in this study and subsequently molecules 11, 40, 44 and 53 were deleted from the test set since they were falling into outliers i.e., they showed more negative values and removal of these molecules increased the q^2 value. Reported IC₅₀ values of molecules were converted into pIC₅₀ (-log IC₅₀) values and were used as dependent variables in CoMFA and CoMSIA analysis. The pIC₅₀ values spanned a range of 3-log unit's homogenous data set for 3D-QSAR study and subsequent 3D QSAR models were generated using a training set of 58

molecules. Predictive powers of the resulting models were evaluated using a test set of 19 molecules. The test set compounds were selected manually such that the

structural diversity and wide range of activity in the data set were included. The structures of the compounds and their biological data are given in Table 1.

Table 1: Structural and activities of Quinazolinone derivatives used for developing CoMFA and CoMSIA models



Compound	n	X	Y	R1	R2	IC ₅₀ (nM)	pIC ₅₀	CoMFA		CoMSIA	
								Predicted	Residual	Predicted	Residual
1	0	H	H	H	H	940	6.03	6.077	-0.051	6.047	-0.021
2	0	H	H	H	<i>o</i> -Cl	510	6.29	6.134	0.158	6.204	0.008
3*	0	H	H	H	<i>p</i> -Cl	370	6.43	6.01	0.42	6.04	0.39
4	0	H	H	H	<i>p</i> -Me	730	6.14	6.039	0.097	6.061	0.075
5*	0	H	H	H	2,3-Me ₂	95	7.02	6.70	0.32	6.69	0.33
6	0	H	H	H	2,4-Me ₂	640	6.19	6.182	0.011	6.20	-0.007
7	0	H	H	H	3,4-Me ₂	1100	5.96	6.081	-0.123	5.994	-0.036
8*	0	H	H	H	<i>o</i> -OMe	80	7.10	6.87	0.23	6.72	0.38
9	0	H	H	H	<i>m</i> -OMe	1400	5.85	6.194	-0.341	5.938	-0.085
10	0	H	H	H	<i>p</i> -OMe	710	6.15	6.155	-0.007	6.156	-0.008
13	0	H	H	H	<i>p</i> -Ac	9000	5.05	5.468	-0.423	5.029	0.016
14	0	H	H	<i>p</i> -F	H	680	6.17	6.126	0.041	6.131	0.036
15	0	H	H	<i>p</i> -F	2,4-Me ₂	500	6.30	6.266	0.035	6.30	0.001
16	0	H	H	<i>p</i> -F	2,6-Me ₂	500	6.30	6.325	-0.024	6.358	-0.057
17	0	H	H	<i>p</i> -F	<i>p</i> -OMe	2500	5.60	5.332	0.027	5.599	0.003
18*	0	H	H	<i>p</i> -F	<i>o</i> -OEt	1300	5.89	6.17	-0.28	6.31	-0.42
19*	0	H	H	<i>p</i> -F	<i>p</i> -NO ₂	7300	5.14	5.61	-0.47	5.46	-0.32
20*	1	H	H	H	H	650	6.19	6.61	-0.42	6.41	-0.22
21	1	H	H	H	<i>o</i> -F	400	6.40	6.675	-0.278	6.531	-0.134
22*	1	H	H	H	<i>p</i> -F	2400	5.62	6.09	-0.47	6.03	-0.41
23	1	H	H	H	<i>o</i> -Cl	130	6.88	6.634	0.246	6.679	0.201
24	1	H	H	H	<i>m</i> -Cl	110	6.90	6.741	0.217	6.849	0.109
25	1	H	H	H	<i>p</i> -Cl	450	6.35	6.303	0.043	6.305	0.041
26	1	H	H	H	3,4-Cl ₂	160	6.80	6.656	0.139	6.768	0.027
27	1	H	H	H	2,3-Me ₂	460	6.34	6.493	-0.156	6.368	-0.031
28	1	H	H	H	2,4-Me ₂	690	6.16	6.18	-0.019	6.160	0.001
29	1	H	H	H	2,5-Me ₂	420	6.38	6.495	-0.119	6.398	-0.022
30*	1	H	H	H	3,4-Me ₂	200	6.70	6.36	0.34	6.39	0.31
31*	1	H	H	H	<i>o</i> -OMe	21	7.68	6.26	0.42	7.29	0.39
33*	1	H	H	H	<i>p</i> -OMe	2000	5.70	6.09	-0.39	6.08	-0.38
34	1	H	H	H	<i>o</i> -OEt	26	7.59	7.375	0.21	7.483	0.102
35*	1	H	H	H	<i>m</i> -CF ₃	350	6.45	7.03	-0.58	6.86	-0.41
37	1	H	F	H	H	930	6.03	6.189	-0.158	6.117	-0.086

Table 1: Structural and activities of Quinazolinone derivatives used for developing CoMFA and CoMSIA models (Contnd)

Compound	n	X	Y	R1	R2	IC ₅₀ (nM)	pIC ₅₀	CoMFA		CoMSIA	
								Predicted	Residual	Predicted	Residual
38	1	H	F	H	<i>o</i> -F	770	6.11	6.506	-0.393	6.306	-0.193
39	1	H	F	H	<i>p</i> -F	770	6.11	6.488	-0.375	6.389	-0.276
41	1	H	F	H	<i>m</i> -Cl	190	6.72	6.487	0.234	6.538	0.183
42*	1	H	F	H	<i>p</i> -Cl	2200	5.66	5.97	-0.31	6.04	-0.38
43	1	H	F	H	3,4-Cl ₂	450	6.35	6.249	0.097	6.262	0.084
45	1	H	F	H	2,4-Me ₂	940	6.03	5.962	0.064	5.952	0.074
46*	1	H	F	H	2,5-Me ₂	1500	5.82	6.17	-0.35	6.26	-0.44
47	1	H	F	H	3,4-Me ₂	590	6.23	6.078	0.151	6.133	0.096
48	1	H	F	H	<i>o</i> -OMe	85	7.07	6.651	0.419	6.765	0.305
50	1	H	F	H	<i>p</i> -OMe	1100	5.96	6.038	-0.080	5.90	0.058
51	1	H	F	H	<i>o</i> -OEt	19	7.72	7.229	0.492	7.48	0.241
52	1	H	F	H	<i>m</i> -CF ₃	92	7.04	6.863	0.173	6.898	0.138
54	1	F	H	H	H	470	6.33	6.579	-0.252	6.516	-0.189
55*	1	F	H	H	<i>o</i> -F	1000	6.00	6.49	-0.49	6.52	-0.52
56	1	F	H	H	<i>p</i> -F	420	6.38	6.499	-0.123	6.44	-0.064
57	1	F	H	H	<i>o</i> -Cl	200	6.7	6.883	-0.185	6.84	-0.142
58	1	F	H	H	<i>m</i> -Cl	130	6.89	6.98	-0.094	7.015	-0.129
59*	1	F	H	H	<i>p</i> -Cl	1200	5.92	6.36	-0.44	6.34	-0.42
60	1	F	H	H	3,4-Cl ₂	270	6.57	6.627	-0.059	6.624	-0.056
61*	1	F	H	H	2,3-Me ₂	55	7.26	6.94	0.32	6.97	0.29
62	1	F	H	H	2,4-Me ₂	620	6.21	6.395	-0.188	6.359	-0.152
63	1	F	H	H	2,5-Me ₂	200	6.70	6.533	0.165	6.578	0.12
64	1	F	H	H	3,4-Me ₂	260	6.59	6.418	0.167	6.525	0.06
65	1	F	H	H	<i>o</i> -OMe	120	6.92	7.158	-0.238	7.114	-0.194
66*	1	F	H	H	<i>m</i> -OMe	920	6.04	6.33	-0.29	6.47	-0.43
67	1	F	H	H	<i>p</i> -OMe	350	6.45	6.121	0.334	6.237	0.218
68	1	F	H	H	<i>o</i> -OEt	12	7.92	7.646	0.274	7.817	0.103
69	1	F	H	H	<i>m</i> -CF ₃	74	7.13	7.498	-0.368	7.30	-0.170
70	1	F	H	H	<i>p</i> -Ac	590	6.23	6.477	-0.248	6.312	-0.083
71	1	H	H	<i>o</i> -OMe	<i>o</i> -OMe	210	6.68	6.869	-0.192	6.793	-0.116
72	1	H	H	<i>o</i> -OMe	<i>o</i> -OEt	29	7.54	7.542	-0.005	7.61	-0.073
73	1	H	F	<i>o</i> -OMe	<i>o</i> -OEt	110	6.96	7.087	-0.129	6.986	-0.028
74	1	F	H	<i>o</i> -OMe	<i>o</i> -OMe	79	7.10	6.872	0.23	6.971	0.131
75	1	F	H	<i>o</i> -OMe	<i>o</i> -OEt	48	7.32	7.458	-0.14	7.484	-0.166
76	1	H	H	<i>m</i> -OMe	<i>o</i> -OMe	98	7.01	7.236	-0.228	7.092	-0.084
77	1	H	H	<i>m</i> -OMe	<i>o</i> -OEt	55	7.26	7.32	-0.061	7.193	0.066
78	1	H	F	<i>m</i> -OMe	<i>o</i> -OEt	91	7.04	7.663	-0.623	7.375	0.335
79*	1	F	H	<i>m</i> -OMe	<i>o</i> -OMe	230	6.64	6.91	-0.27	7.03	-0.39
80	1	F	H	<i>m</i> -OMe	<i>o</i> -OEt	16	7.80	7.363	0.432	7.518	0.277
81	1	H	H	<i>p</i> -OMe	<i>o</i> -OMe	97	7.01	7.188	-0.175	7.001	0.012
82	1	H	H	<i>p</i> -OMe	<i>o</i> -OEt	29	7.54	7.437	0.100	7.416	0.121
83	1	H	F	<i>p</i> -OMe	<i>o</i> -OEt	49	7.31	7.261	0.048	7.216	0.093
84*	1	F	H	<i>p</i> -OMe	<i>o</i> -OMe	190	6.72	7.14	-0.42	7.17	-0.45
85	1	F	H	<i>p</i> -OMe	<i>o</i> -OEt	16	7.80	7.892	-0.097	7.936	-0.141

Compounds marked as (*) belong to test set

Molecular alignment

CoMFA results are extremely sensitive to a number of factors such as alignment rules, overall orientation of the aligned compounds, lattice shifting - step size and probe atom type. The accuracy prediction of CoMFA models and the reliability of contour models depend strongly on the structural alignment of the molecules. Therefore, we applied molecular alignment tool in SYBYL 6.7 to align all the molecules used in the present study based on a common scaffold. The initial structures were minimized using Tripos force field besides assigning Gasteiger-Hückel charges using conjugate gradient method, and convergence criterion was set to 0.005kcal/mol. The most active compound 68 was used as an alignment template upon which the rest of the molecules were aligned to it by using the common substructure (Figure 1).

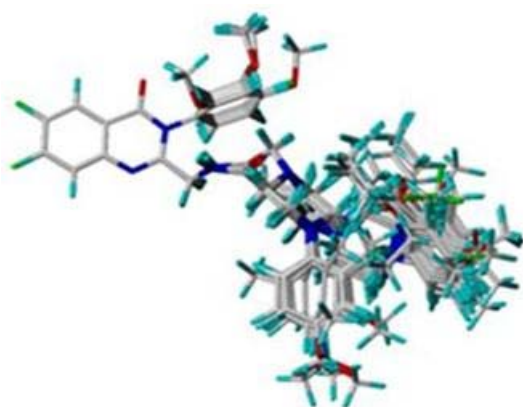


Figure 1: Superposition of all Quinazolinones molecules with common scaffold

Predictive r-squared

To validate the derived CoMFA and CoMSIA models, biological activities of an external test set of nineteen compounds (Table 1) were predicted using models derived from the training set. The predictive ability of the models is expressed by the predictive r^2 value, which is analogous to cross-validated r^2 (q^2) and is calculated using the formula.

$$r_{pred}^2 = \frac{SD - PRESS}{SD}$$

SD is the sum of the squared deviations between the biological activities of the test set molecules and PRESS is the sum of the squared deviations between the observed and the predicted activities of the test molecules.

CoMFA studies

Steric and electrostatic interactions were calculated using Tripos force field¹³ with a distance-dependent dielectric constant at all interactions in a regularly spaced (2Å) grid taking a sp^3 carbon atom as steric probe and a $+1$ charge as electrostatic probe. The cutoff was set to 30kcal/mol. With standard options for scaling of variables, the regression analysis was carried out using fully cross-validated partial least squares (PLS) method (leave-one-

out).¹⁴ The minimum sigma (column filtering) was set to 2.0kcal/mol to improve signal to noise ratio by omitting those lattice points whose energy variation was below this threshold. The final model which is non cross-validated conventional analysis was developed with the optimum number of components to yield a non cross-validated r^2 value.

CoMSIA studies

In CoMSIA, a distance-dependent Gaussian-type physicochemical property has been adopted to avoid singularities at the atomic positions and dramatic changes to potential energy for those grids in the proximity of the surface. With these standard parameters and no arbitrary cutoff limits, five physic-chemical properties, namely, steric, electrostatic, hydrophobic, hydrogen bond donor and hydrogen bond acceptor fields were calculated. The steric contribution was reflected by the third power atomic radii of the atoms. Electrostatic properties were introduced as atomic charges resulted from molecular docking. An atom-based hydrophobicity was assigned according to the parameterization developed by Gholke et al.¹⁵ The lattice dimensions were selected with a sufficiently large margin (>4Å) to enclose all the binding conformations of the inhibitors. In general, similarity indices, $A_{F, k}$ between the compounds of interest were computed by placing a probe atom at the intersections of the lattice points using Equation 1.

$$A_{F, k}^q(j) = -\sum W_{probe, k} W_{ik} e^{-a r_{iq}^2}$$

Where q represents a grid point, i is the summation index over all atoms of the molecule j under computation, W_{ik} is the actual value of the physicochemical property k of atom i , and $W_{probe, k}$ is the value of the probe atom. In the present study, we used a probe atom ($W_{probe, k}$) with charge +1, radius 1Å, hydrophobicity +1, and attenuation factor of 0.3 for the Gaussian type distance. The statistical evaluation for the CoMSIA analysis was performed in the same way as described for CoMFA.

Partial least squares (PLS) analysis

PLS (partial least squares) method¹⁶ was used to linearly correlate the CoMFA fields to biological activity values. The cross-validation was performed using leave-one-out (LOO) method in which one compound is removed from the dataset and its activity is predicted using the model derived from the rest of the molecules in the dataset. Equal weights for CoMFA were assigned to Steric and Electrostatic fields using CoMFA STD scaling option. To speed up the analysis and to reduce noise, a minimum column filter value of 2.0kcal/mol was used for the cross-validation. Non-cross-validation was performed to calculate conventional r^2 using the same number of components. To further assess the robustness and statistical confidence of the derived models, bootstrapping analysis for 100 runs was performed.¹⁷ Bootstrapping involves generation of many new data sets from original dataset and is obtained by randomly choosing samples from the original dataset. The statistical

calculation is performed on each of these bootstrapping sampling. The difference between the parameters calculated from the original dataset and the average of the parameters calculated from many bootstrapping samplings is a measure of the bias of the original calculations. The entire cross-validated results were analyzed considering the fact that a value of q^2 above 0.3 indicates that probability of chance correlation is less than 5%.

RESULTS AND DISCUSSION

3D-QSAR analysis

CoMFA and CoMSIA 3D-QSAR models were derived using previously reported 5-HT₇ inhibitors. The chemical structures of molecules and their experimental biological activity (IC₅₀) values are shown in Table 1.

CoMFA analysis

Fifty eight compounds out of seventy seven Quinazolinone derivatives were used as training set and nineteen compounds were used as test set. PLS analysis was carried out for the training set and a cross-validated q^2 of 0.851 for five components was obtained. The non cross-validated PLS analysis with the optimum components revealed a conventional r^2 value of 0.950, F value = 197.312 and standard error of estimate (SEE) 0.140. The Steric field descriptors explain 56.8% of variance, while the electrostatic descriptors explain 43.2% of the variance. Bootstrap analysis for 100 runs was then carried out for further validation of the model by statistical sampling of the original dataset to create new datasets.

Table 2: CoMFA and CoMSIA statistical analyses for Quinazolinone derivatives as 5HT₇ receptors

Component	CoMFA	CoMSIA
q^2	0.851	0.850
r^2	0.950	0.945
Number of components	5	6
F-Value	197.312	146.683
SEE	0.140	0.148
Cross validation	0.858	0.867
r^2 pred	0.700	0.702
Field Contribution (%)		
Steric	56.8	22.3
Electrostatic	43.2	40.6
Hydrophobic		27.6
Hydrogen bond donor		8.4
Hydrogen bond acceptor		1.2

Thus, the difference in the parameters calculated from the original data and the average of the parameters calculated from the N (=100) runs of bootstrapping sampling is a measure of the bias of the original calculation. This yielded higher $r^2_{\text{bootstrap}}$ value 0.958 for

CoMFA with standard error value of 0.124. This further supports the statistical validity of the developed models. The predicted activities for the derivatives versus their experimental values are listed in Table 1 and the correlation between the predicted activities and the experimental values is depicted in Figure 2(a). Illustrate the predicted activities using the CoMFA model are in good agreement with the experimental data, suggesting that the CoMFA model should have a satisfactory predictive ability. The PLS analysis results of CoMFA are summarized in Table 2.

CoMSIA analysis

A CoMSIA analysis was performed using five descriptor fields: Steric, Electrostatic, Hydrophobic, Hydrogen bond donor and acceptor. The CoMSIA study revealed a cross validate q^2 of 0.850 with 6 as optimum number of components, a conventional r^2 of 0.945 with standard error of estimate 0.148 and F value 146.683 for training set. The Steric field descriptor explains 22.3% of the variance and the electrostatic descriptor explains 40.6%, the hydrophobic field explains 27.6% while hydrogen bond donor explains 8.4% and hydrogen bond acceptor explains 1.2% of variance.

Bootstrap analysis for 100 runs was then carried out for further validation of the model by statistical sampling of the original dataset to create new datasets. Thus, the difference in the parameters calculated from the original data and the average of the parameters calculated from N (=100) runs of bootstrapping sampling is a measure of the bias of the original calculation. This yielded higher $r^2_{\text{bootstrap}}$ value 0.961 for CoMSIA with standard error value of 0.124 supporting the statistical validity of the developed models. The correlation between the experimental and predicted bioactivities is shown in Figure 2(b). Results show that prediction by the CoMSIA model is reasonably accurate. The PLS analysis results CoMFA are summarized in Table 2.

Validation of 3D-QSAR models

The nineteen manually selected compounds were used as testing set to verify the stability and predictive ability of the CoMFA and CoMSIA models. The predicted pIC₅₀ with the QSAR models are in good agreement with the experimental data within a statistically tolerable error range, with a predicted correlation coefficient r^2_{pred} = 0.789 and 0.730 for CoMFA and CoMSIA, respectively. The correlation between CoMFA and CoMSIA predicted activities and the experimental activities of the test set compounds are depicted in Figure 2. The testing results indicate that the CoMFA and CoMSIA models can be reliably used in the design of novel Quinazolinone derivatives.

CoMFA and CoMSIA contour analysis

The CoMFA Steric and Electrostatic fields from the final non-cross-validated analysis were plotted as 3-D colored contour maps Figure 3(a) and 3(b) the field energies at each lattice point were calculated as the scalar results of

the coefficient and the standard deviation associated with a particular column of the data table ($SD \cdot \text{coeff}$), always plotted as the percentages of the contribution of CoMFA equation. These maps show regions where differences in molecular fields are associated with differences in biological activity. The CoMFA and CoMSIA contours for Steric and Electrostatic fields are shown in Figure 3(a) and 3(b), and CoMSIA Hydrophobic, Hydrogen bond donor and Hydrogen bond acceptor fields are shown in Figures 4 (a) and (b), respectively. In these contour maps, each colored contour represents particular properties such as green contours for regions of high Steric tolerance (80% contribution), yellow for low Steric tolerance (20% contribution), red contours for regions of decreased Electrostatic tolerance for positive charge (20% contribution), blue for regions of decreased Electrostatic tolerance for negative charge (80% contribution), yellow contours represent Hydrophobically favored regions (80% contribution) and white contours for Hydrophobically disfavored regions (20% contribution). The magenta and red contours denote favorable and unfavorable regions for hydrogen bond acceptor respectively whereas cyan and purple contours represents favorable and unfavorable regions for Hydrogen bond donor groups, respectively.

Steric contour derived from inhibitory biological activity data of Quinazolinones derivatives using CoMFA method is displayed in Fig. 3(a). Green colored isopleths displayed in figure corresponds regions, where the presence of bulky Steric groups is favored and should enhance 5-HT₇ inhibitory activity of molecule. On the other hand, areas indicated by yellow isopleths correspond to regions for unfavorable presence of steric groups and should be avoided for better activity of molecule. In Fig. 3(a), for the highest active molecule 68, favorable green region is present close to ortho attached to one of the benzene ring, indicating that any bulkier substituent is preferred at this position for higher activity. Unfavorable yellow isopleths are also present at the benzene ring, indicating crucial role of bulky substitution at this position. Accordingly, in the highest active molecule 68 ortho substituted OEt group is oriented into sterically favorable green region. In other highly active molecules 34, 51, 65, 72, 75, 80, 82 and 85 sterically favorable ortho substituent's are also oriented towards green regions. In the lowest active molecules 18, substituent at ortho position is very bulky and orients into sterically unfavorable yellow isopleths.

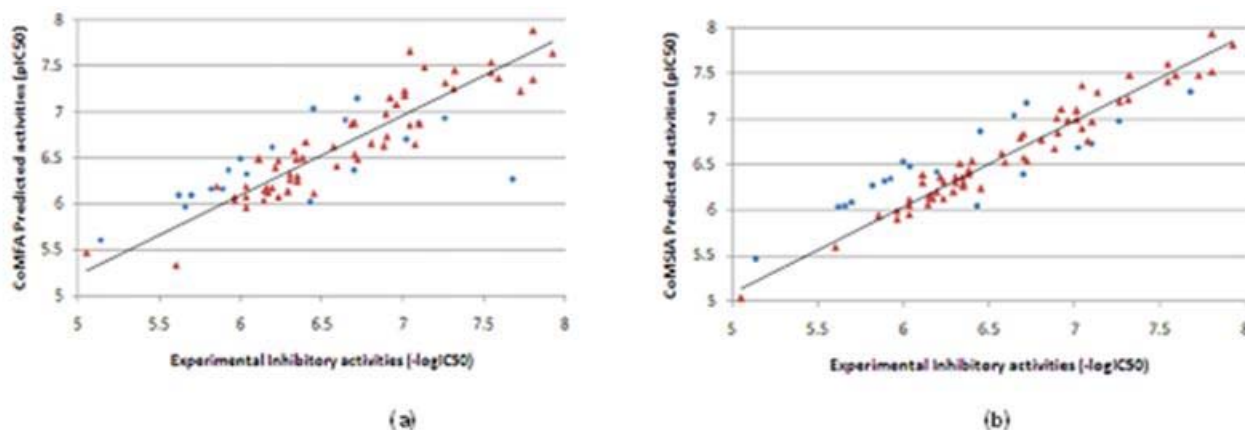


Figure 2: (a) are the predictive versus experimental pIC_{50} values derived from CoMFA model for training set (red triangle) and test set (blue round); (b) are the predictive versus experimental pIC_{50} values derived from CoMSIA model for training set (red triangle) and test set (blue round).

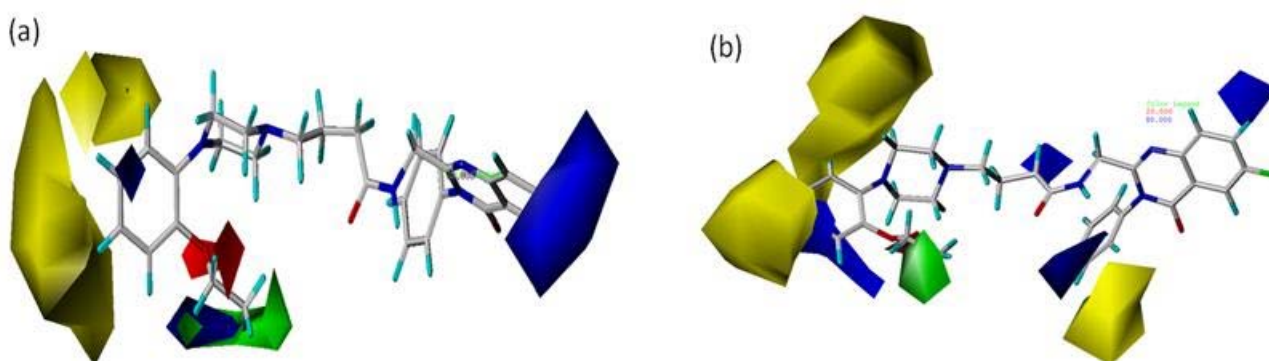


Figure 3: Contour plot showing CoMFA and CoMSIA (a) CoMFA Steric and electrostatic fields (b) CoMSIA steric and Electrostatic fields. [Note: green – favored steric groups; yellow – disfavored steric groups; blue - Favored for electropositive groups; red - disfavored of electropositive groups.]

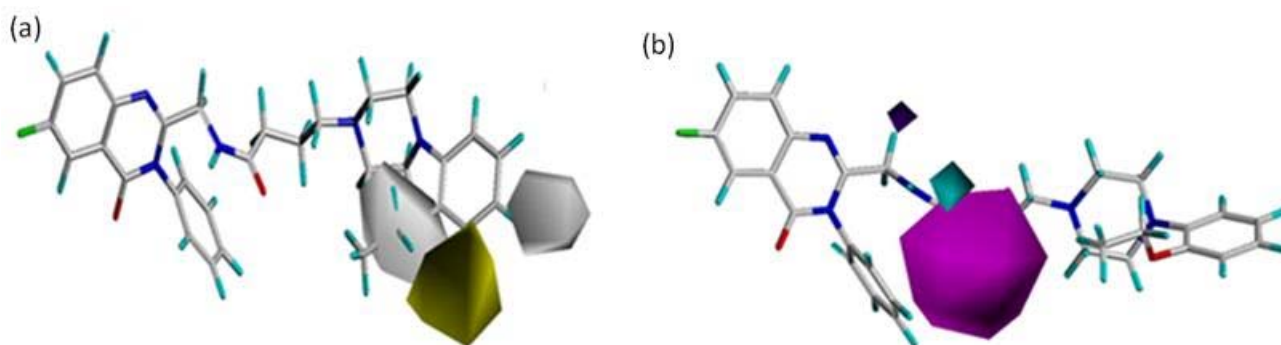


Figure 4: (a) CoMSIA hydrophobic field Contour plot for molecule 68; yellow - favored; white – disfavored; (b) CoMSIA hydrogen bond donor and acceptor field Contour plot for molecule 68; cyan - favored for H-bond donor; magenta - favored for H-bond acceptor field Contour plot for molecule 68; yellow - favored; white – disfavored.

Electrostatic CoMFA contour map analysis is displayed in Figure 3(a). More electropositive substituents are predicted to be favored in blue areas whereas electronegative into red regions. In Figure 3(a), the highest active molecule orients its substitutions correctly into corresponding regions. A red isopleth is present near *o*-OEt group of the benzene ring indicates that the electronegative group is favorable at these positions. In the figure, an electropositive favorable blue isopleth is present close to piperazine ring showing importance of NH group at this position. Two blue isopleths are also present at the ortho position of benzene ring superimposed on the red isopleths; whereas other isopleth is present near at the 38th position of the phenyl ring.

CoMSIA Steric fields are similar to corresponding CoMFA field's even better explanatory as shown in Figure 3(b). In both CoMFA and CoMSIA contour maps, one green and one yellow contour of CoMSIA Steric map can be well compared with Steric contour maps. In CoMSIA Steric contour for molecule 68, a large unfavorable yellow region is present near the benzene ring, indicating the unfavorable conditions for bulky group substitution at this position. Figure 4(a) shows the hydrophobic CoMSIA contour maps analysis in which yellow favorable isopleths indicates favorable and white isopleths indicate disfavored regions for hydrophobic groups in respective regions.

The electrostatic contours of CoMSIA in Fig. 3(b) shows that the pattern of electropositive favorable blue and electronegative favorable red regions can be well compared with that of the electrostatic contour maps of CoMFA shown in Fig. 3(a). In both CoMFA and CoMSIA contour maps, a red and two blue isopleths are present close to the ortho position of benzene ring close to OEt group at piperazine ring. A red area is present at ortho position of benzene ring showing favor for presence of electronegative groups at this position like in molecules 51, 57, 65, 75 and 80. One large blue isopleth is present near the 14th position of benzene ring showing favorable presence of electropositive group at this position. Other electropositive favorable blue isopleths are present near

the 8th, 34th and 38th position of the ring explaining high activity of molecules 80 and 85.

In the most active molecule 68, a yellow isopleth present near the 14th position of benzene ring favors the presence of the hydrophobic group at this position. In compounds 34, 51, 75, 80, 82 and 83 the favorable hydrophobic group is also present at the same position. Low activity of molecules 8, 18, 57, 65, 73 and 78 is due to the presence of hydrophobic groups oriented toward unfavorable white isopleths. Two white isopleths positioned near the benzene ring shows the favorable hydrophilic group at this position and this can be explained on the basis of the resonance of carbonyl group with benzene ring which make the ring polar and favors the positioning of phenyl and carbonyl group at this position for activity.

In figure 4 (b) Hydrogen-bond donor and acceptor contour maps from CoMSIA are shown in Magenta isopleth favors the positioning of the hydrogen bond acceptor group in these regions whereas red isopleth disfavors the presence of H-bond acceptor groups. The hydrogen-bond acceptor contour map is shown with a big magenta contour region in which the hydrogen-bond acceptor is favored. The magenta region is mainly present at the 8th position of the 'O' substitution. There is no presence of red isopleth indicating that there is no H-bond acceptor group which disfavors these regions. Contours for hydrogen bond donor property are displayed. In this contour map cyan color favors the presence of h-bond donor groups whereas purple color disfavors. The contour map shows a small cyan region at the 8th and 9th position on the ring, which is generally considered as the favorable regions for hydrogen bond donor groups.

CONCLUSION

In this study, 3-D CoMFA and CoMSIA QSAR analysis were used to predict the antidepressant activity of Quinazolinones. The QSAR models gave good statistical results in terms of q^2 and r^2 values. The CoMFA model provided the most significant correlation of Steric and Electrostatic fields with the biological activities. Overall, the CoMFA and CoMSIA provided a better statistical

model, which implies the significance of Steric and Electrostatic fields in the selectivity and activity of these compounds. The statistical significance and robustness of the 3D-QSAR models generated were confirmed by using a test set. The effects of the Steric, Electrostatic, and Hydrophobic fields around the aligned molecules on their activities were clarified by analyzing the CoMFA and CoMSIA contour maps. The information from this study suggests that incorporating bulk, higher degree of electro negativity, and Hydrophilicity on basic amino side chain, along with diminishing steric bulk and electro negativity on 15, 16th position of benzene ring, might be favorable for better antidepressants agents. It can be noted that Quinazolinones with the requisite groups could serve as a privileged structure of exploring antidepressant agents. In the future information elaborated by these models can be exploited to design new 5-HT₇ inhibitors with improved potency and to predict their activity prior to synthesis.

REFERENCES

1. Hoyer D, Hannon JP, Martin GR, Molecular, pharmacological and functional diversity of 5-HT receptors, *Pharmacol Biochem Behavior*, 71, 2002, 533-554.
2. Meng EC, Bourne HR, Receptor activation: what does the rhodopsin structure tell us? *Trends Pharmacol Sci*, 22, 2001, 587-593.
3. Kroeze WK, Kristiansen K, Roth BL, Molecular biology of serotonin receptors structure and function at the molecular level, *Curr Top Med Chem*, 2, 2002, 507-528.
4. Kristiansen K, Molecular mechanisms of ligand binding, signaling, and regulation within the superfamily of G-protein-coupled receptors: molecular modeling and mutagenesis approaches to receptor structure and function, *Pharmacol Ther*, 103, 2004, 21-80.
5. Kroeze WK, Sheffler DJ, Roth BL, G-protein-coupled receptors at a glance, *J Cell Sci*, 116, 2003, 4867-4869.
6. Bhalla P, Saxena PR, Sharma HS, Molecular cloning and tissue distribution of mRNA encoding porcine 5-HT₇ receptor and its comparison with the structure of other species, *Mol Cell Biochem*, 238, 2002, 81-88.
7. Plassat JL, Amlaiky N, Hen R, Molecular cloning of a mammalian serotonin receptor that activates adenylate cyclase, *Mol Pharmacol*, 44, 1993, 229-236.
8. Shen Y, Molecular cloning and expression of a 5-hydroxytryptamine₇ serotonin receptor subtype, *J Biol Chem*, 268, 1993, 18200-18204.
9. Vanhoenacker P, Haegeman G, Leysen JE, 5-HT₇ receptors: current knowledge and future prospects, *Trends Pharmacol Sci*, 21, 2000, 70-77.
10. Cramer RD, Patterson DE, Bunce JD, Comparative molecular field analysis (CoMFA). 1. Effect of shape on binding of steroids to carrier proteins, *J Am Chem Soc*, 110, 1988, 5959-5967.
11. Klebe G, Abraham U, Mietzner T, Molecular similarity indices in a comparative analysis (CoMSIA) of drug molecules to correlate and predict their biological activity, *J Med Chem*, 37, 1994, 4130-4146.
12. Na YH, Novel quinazolinone derivatives as 5-HT₇ receptor ligands, *Bioorg Med Chem*, 16, 2008, 2570-2578.
13. Clark M, Richard i, Cramer D, Opdenbosch NV, Validation of the general purpose Tripos 5.2 force field, *J. Comput. Chem*, 10, 1989, 982-1012.
14. Geladi P, Kowalski BR, Partial least-squares regression: a tutorial, *Analytica Chimica Acta*, 185, 1986, 1-17.
15. Gohlke H, Hendlich M, Klebe G, Knowledge-based scoring function to predict protein-ligand interactions, *J Mol Biol*, 295, 2000, 337-356.
16. Cramer RD, Crossvalidation, Bootstrapping, and Partial Least Squares Compared with Multiple Regression in Conventional QSAR Studies, *Quantitative Structure-Activity Relationships*, 7, 1988, 18-25.
17. Bush BL, Nachbar RB, Sample-distance partial least squares: PLS optimized for many variables, with application to CoMFA, *J Comput Aided Mol Des*, 7, 1993, 587-619.

Source of Support: Nil, Conflict of Interest: None.

